Asian Journal of Chemistry; Vol. 35, No. 9 (2023), 2275-2284

ASIAN JOURNAL OF CHEMISTRY

https://doi.org/10.14233/ajchem.2023.28239

Visible and Solar Light Degradation of Ciprofloxacin and Norfloxacin using Titania Nanocomposite

M. VIJAYATHA[1], B. VIJAYALAXMI[1], MD. SAJEEDA[1], B. RAVALI[1], K. VENKATESHAM[1], M. KALPANA[2], B. PADMA[1] and A. HARI PADMASRI[1,*]

[1]Department of Chemistry, University College of Science, Osmania University, Hyderabad-500007, India
[2]Catalysis & Fine Chemicals Department, CSIR-Indian Institute of Chemical Technology, Hyderabad-500007, India

*Corresponding author: E-mail: ahpadmasri@osmania.ac.in; ahpadmasri@gmail.com

Received: 30 June 2023; *Accepted*: 16 August 2023; *Published online*: 31 August 2023; AJC-21375

A simple sol-gel approach was used to synthesize TiO_2 nanoparticles and its composite TiO_2-PEG (TPG) using polyethylene glycol (PEG). The synthesized samples were characterized by XRD, SEM -EDX, TEM, UV-DRS, photoluminescence, Raman, XPS and BET-surface area techniques. The development of non-toxic, cost-effective, biocompatible and efficient polymeric nanocomposite increases the mechanical, thermophysical and physico-chemical properties of prepared nanomaterials. PEG affected the reaction with the crystallization process of the prepared titania nanoparticles to a great extent. The antibiotics ciprofloxacin and norfloxacin of fluoroquinolone class are widely used to treat certain bacterial infections and at the same time their residues generate serious health issues due to the lack of proper waste water treatment systems thus causing environmental pollution. The present study is thus focused on synthesizing efficient titania PEG nanocomposite to enhance the photocatalytic degradation of antibiotics in both solar and visible light. Efficiency of degradation was achieved maximum upto 74% with TPG and 64% with pure TiO_2 nanoparticles for ciprofloxacin in visible light, similarly the degradation of norfloxacin was achieved 65% with TPG and 57% with TiO_2 nanoparticles. Sunlight irradiation resulted in the degradation of ciprofloxacin to 80.2% with TPG and 77% with TiO_2 nanoparticles whereas it was 78.7% with TPG and 68.6% with TiO_2 nanoparticles for the degradation of norfloxacin. These results indicate that the catalyst TPG showed higher activity in presence of solar and visible light than TiO_2 nanoparticles. Recyclability was also studied showing the stability of the photocatalyst used even after five successive runs.

Keywords: Nanocomposites, Polyethylene glycol, Biocompatibility, Photocatalysis, Degradation, Ciprofloxacin, Norfloxacin.

INTRODUCTION

Titanium dioxide (TiO_2) in its nano form is widely used photocatalyst for environmental remediation due to its high stability, anticorrosive and photocatalytic properties [1]. Inorganic nanoparticles well dispersed in organic polymer matrix help in building up nanocomposites [2]. The optical, electrical, thermal and mechanical properties get enhanced by using nanocomposites [3]. The recent advances include modification of metal oxide and shielding the surface charge of nanoparticles, which can be achieved by coating the surface using biocompatible polymers like polyvinyl alcohol, polyacrylamides, polysaccharides, poly-*N*-vinyl 2-pyrrolidone, polyethylene glycol (PEG), *etc*. for additional stability.

Large-scale use of antibiotics poses a major threat to ecosystem and human health, hence several techniques are employed to eliminate them namely biological treatments [4], membrane processes [5], chemical and electrochemical methods [6,7] and adsorption experiments [8]. However, antibiotics as small traces in wastewater cannot be completely eliminated by most of these techniques due to their complex nature or may require large spaces. Researchers tried nanocomposites for the removal of antibiotics from the environment [9,10]. Semiconductor photocatalysts used in advanced oxidation processes (AOPs) serves as the most advantageous method in this regard hence attaining great attention [11,12].

Major pollutants like organic compounds and inorganic ions degradation using TiO_2 as photocatalyst has attracted great interest [13]. Surface modification using polymer and doping with metallic or non-metallic ions improves the photocatalytic performance of TiO_2, as it is greatly restricted by its wide band-gap energy (3.2 eV) and high recombination rate of electron-hole pair [14]. Water soluble anatase TiO_2 nanoparticles can be successfully synthesized with the use of a surfactant such as ethylene glycol [15].

Polyethylene glycol (PEG) is hydrophilic and able to stabilize nanoparticles by steric and non-ionic effects in water [16,17]. PEGylation of inorganic nanoparticles has several advantages in biomedical fields like drug delivery, imaging and therapeutics [18]. Solubility of metal oxide clusters in the melt of PEG helps in proton conduction forming nanocomposites thus promoting conduction of protons under ambient conditions [19]. PEG-400 use as a solvent and a stabilizer is even well established in the successful synthesis of nanoparticles with HCl in the reaction system to control the phase transformation [20]. Photocatalytic activity of TiO_2 nanoparticles increases with the increasing molecular weight in PEG molecules [21].

The synthesis of nanocomposite proved to be efficient in photocatalytic degradation of ciprofloxacin and norfloxacin, which are the common drugs responsible for water system contamination [22]. The present work aims to synthesize titania nanoparticles by employing the sol-gel method and modifying nanoparticles prepared by adding PEG to TiO_2 sol [23]. The samples of TiO_2 nanoparticles and TiO_2-PEG nanocomposite were then investigated by various characterization techniques and a comparative study was done showing the differences in size and morphology of pure TiO_2 nanoparticles with PEG-TiO_2 nanocomposite. The prepared catalysts were then analyzed for their photocatalytic efficiency in the degradation study of ciprofloxacin and norfloxacin under the irradiation of both solar and visible light. The present work has demonstrated that the activity of the catalyst in the breakdown of antibiotics is significantly improved by the use of surface modified TiO_2 composites, in contrast to simple TiO_2 nanoparticles.

EXPERIMENTAL

Titanium tetra isopropoxide ($Ti(OCH(CH_3)_2)_4$, (NRchem), urea (NH_2CONH_2, AVRA), polyethylene glycol (*m.w.* 4000, SD Fine Chemicals, India), ciprofloxacin ($C_{17}H_{18}FN_3O_3$) and norfloxacin ($C_{16}H_{18}FN_3O_3$) (Sigma-Aldrich, purity > 98%) were used as received.

Synthesis of TiO_2 nanoparticles: Titania nanoparticles were synthesized by adopting sol-gel procedure using titania tetra isopropoxide (TTIP) as precursor. The hydrolysis step involved the utilization of a urea solution, to which a TTIP solution was gradually introduced with stirring for a duration of 30 min. The obtained suspension was heated on water bath for 1 h at 50 ºC. Product obtained was then filtered and dried in an oven at 60 ºC and finally calcined at 400 ºC for 5 h.

Synthesis of TiO_2–PEG nanocomposite: Sol-gel method was adopted for PEGylation of TiO_2 nanoparticles using hydrolysis and precursor solutions [24]. Hydrolysis solution was prepared using propanol and water with addition of few drops of nitric acid to control pH of the solution. TTIP, propanol and PEG-4000 were used to prepare precursor solution. Both solutions were mixed and heated together till 60-80 ºC while stirring continuously, this condition was continued until sol-gel transformation was complete. This results in the formation of precipitate, which was washed using ethanol and dried at 100 ºC for 12 h resulting in yellow white powder and was annealed finally. The synthesized samples were designated as TiO_2 NP for titania nanoparticles and TPG for TiO_2-PEG nanocomposite.

Characterization: The XRD pattern was obtained for the synthesized catalysts using a Rigaku miniplex Powder X-ray diffractometer operated at 40 kV and 15 mA Cu*K*α (1.5064 Å) radiation source over a range of 20º to 80º to identify the crystallization. The surface area and pore structure of synthesized nanomaterials were studied by N_2 adsorption at -196 ºC using a Micromeritic ASAP 2010 surface area analyzer and specific surface area was calculated using Brunuer, Emmett and Teller method (BET). Carl Zeiss Merlin compact SEM was used to study the morphology of samples and elemental composition was studied using EDX Oxford instrument X-maxN SDD (50 mm^2) system interfaced at 5 kV and INCA analysis software. Particle size distribution of samples was studied using JEM F200 JOEL, 200 kV transmission electron microscope (TEM). UniRAM 3300 micro-Raman mapping spectrometer was used to record Raman spectra of the samples prepared. Elemental composition and valence states of the samples were investigated using KRATOS-AXIS 165 instrument equipped with dual aluminium magnesium anodes using Mg*K*α radiation X-ray photoelectron spectrometer. JASCO V650 UV-Vis spectrophotometer was utilized to record UV-DRS spectra of the samples in the range of 200-800 nm.

Photocatalytic studies: TiO_2 nanoparticles and TiO_2-PEG nanocomposite (TPG) photocatalytic activity was investigated by the degradation of antibiotics ciprofloxacin (CIP) and norfloxacin (NOR) under visible light and solar light irradiation. The photocatalytic activity study was carried out on a 250 W visible lamp reactor supplied by Lelesil innovative system, India. A cylindrical quartz jacketed reactor tube immersion well holds the visible lamp of 250 W for the sample irradiation with a provision of reflectors, cool water circulation, magnetic stirrer and air purging. About 40 mL of aqueous drug solution of an initial concentration (C_o), 50 mg and 75 mg of catalyst were taken in the quartz tube. Then, it was suspended in dark with air purging for 1 h in order to attain adsorption-desorption equilibrium. A millipore filter was used to withdraw about 4 mL of solution to remove any traces of catalyst particles at regular time intervals of 30 min to record the absorbance using an UV-Visible spectrophotometer. The degradation rate of antibiotics was calculated by using the following formula:

$$\text{Degradation } (\%) = \frac{1 - C_f}{C_o} \times 100$$

where C_f and C_o represents the final and initial concentrations of the drug solution.

RESULTS AND DISCUSSION

Powder X-ray diffraction (PXRD) studies: The phase, structure and crystallite size of the samples were studied using PXRD, which was carried out in the range of 2θ = 10º-80º. As observed in Fig. 1, the samples show sharp and intense diffraction peaks suggesting that samples were well-crystallized. The major diffraction peaks at 2θ = 25.3º, 37.7º, 48.06º, 53.88º, 62.9º, 70.06º and 75.38º corresponds to the planes (101), (004),

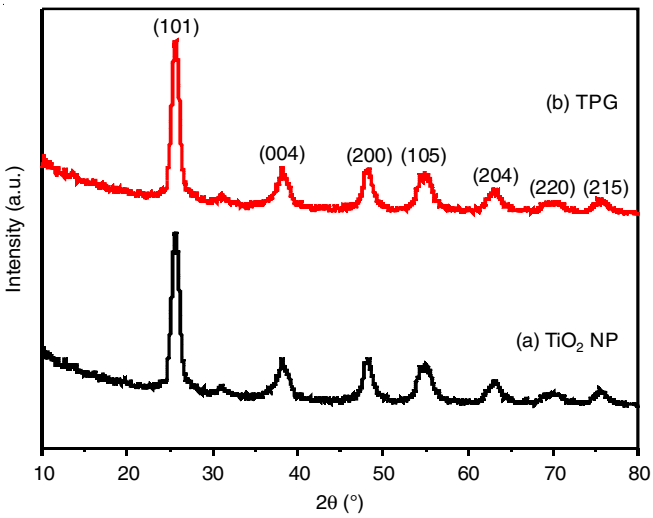

Fig. 1. Powder X-ray diffractograms of the catalysts (a) TiO_2 NP and (b) TPG

(200), (105), (204), (220) and (215) confirmed pure anatase phase with tetragonal structure that matches with JCPDS data (card no. 21-1272). Surface modified TiO_2 with PEG did not alter the structure of TiO_2 nanoparticles thus confirming pure anatase phase without any impurities. Debye Scherrer's formula was used to calculate crystallite size of the catalysts prepared. The observed crystallite size of TiO_2 NPs and TPG was found to be 15.28 nm and 14.93 nm, respectively.

SEM and EDAX studies: The SEM images (Fig. 2) of pure TiO_2 nanoparticles and TiO_2-PEG nanocomposite revealed that the nanocomposites are more spherical in shape with small agglomeration in nano-sized range than pure TiO_2 nanoparticles. The particles were found to be more uniform with PEGlyation as observed from the micrograph image of TPG. The EDAX spectra displayed the elemental composition in the samples in desired amounts.

TEM and SAED studies: TEM image and SAED pattern of TiO_2 nanoparticles and TPG (Fig. 3) show a quasi-spherical morphology with narrow size dispersion characteristic of nanocomposite in polymer matrix such as PEG in TPG. Whereas a non-uniform particle size distribution could be seen with some agglomerization in case of TiO_2 nanoparticles sample. The selected area electron diffraction patterns revealed the ring

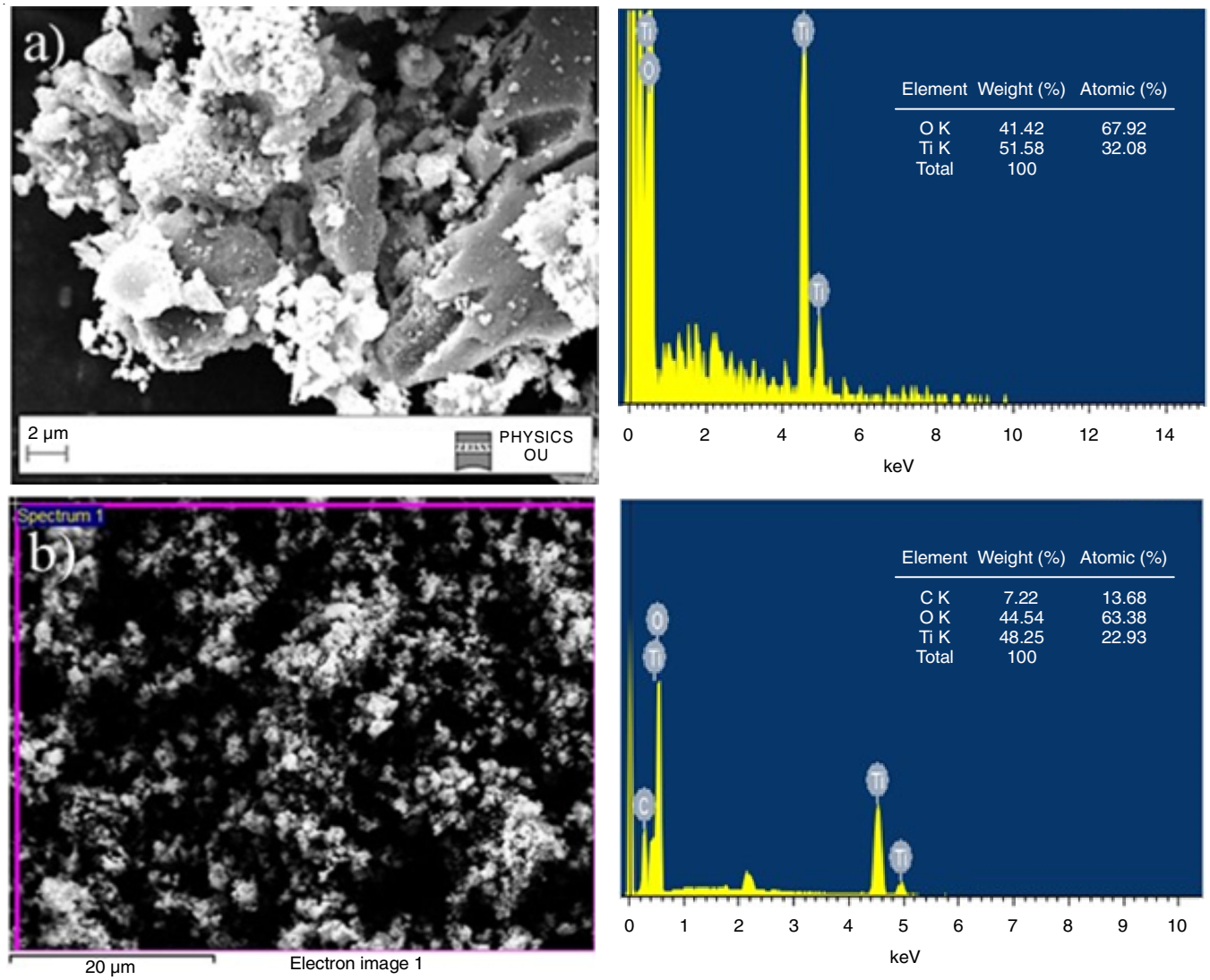

Fig. 2. SEM micrographs and EDAX spectra of (a) TiO_2 NP (b) TPG

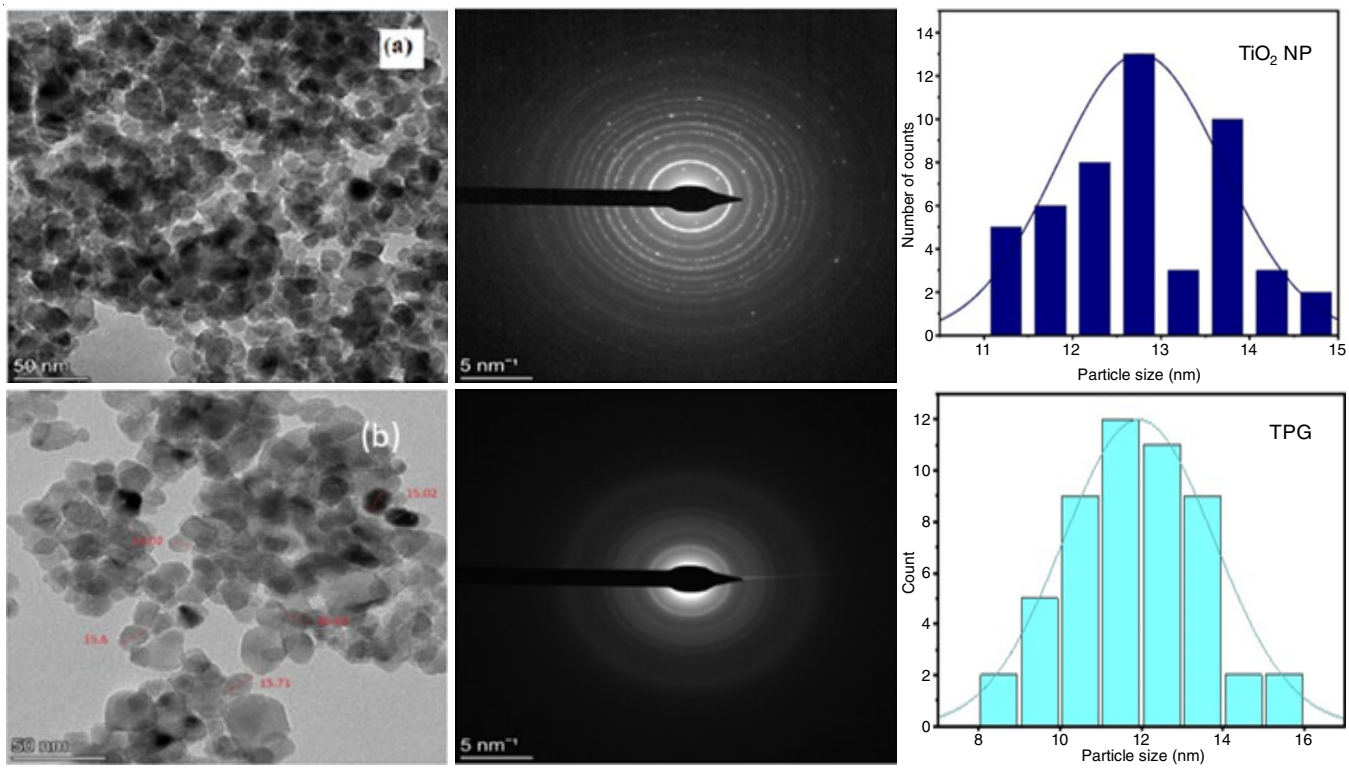

Fig. 3. TEM images, SAED and histograms of the samples (a) TiO_2 NP and (b) TPG

patterns that suggests the polycrystalline nature of catalysts. The average particle size of about 12.7 nm in TiO_2 nanoparticles and about 11.6 nm in TPG was measured. Histograms clearly show the particles to be more uniform in case of TPG unlike the other catalyst.

UV-Vis DRS studies: The UV-Vis absorption spectra (Fig. 4) revealed an absorbance between 330-420 nm range with maximum wavelength at 330.6 nm for TiO_2 nanoparticles and 343.2 nm for TPG with absorption wavelength edge showing a red shift in the wavelength with PEGylation to form nanocomposite. It was further proved by plotting Kubelka Munk plot used for band gap calculation which is 3.09 eV for pure TiO_2 nanoparticles and 2.99 eV for TPG that the band gap energy is lowered for the composite. From the calculated values of band gap energies it is evident that TPG catalyst shows small band gap energy compared with TiO_2 nanoparticles, thus it is more effecient for photocatalytic activity.

Photoluminiscence studies: In determining the effeciency of the photocatalytic materials, the recombination of gererated electron hole pair plays a vital role [25,26]. Photoluminiscence (PL) emission spectra of TiO_2 nanoparticles and TPG exhibits photoluminiscence emission in the range of 630 to 730 nm

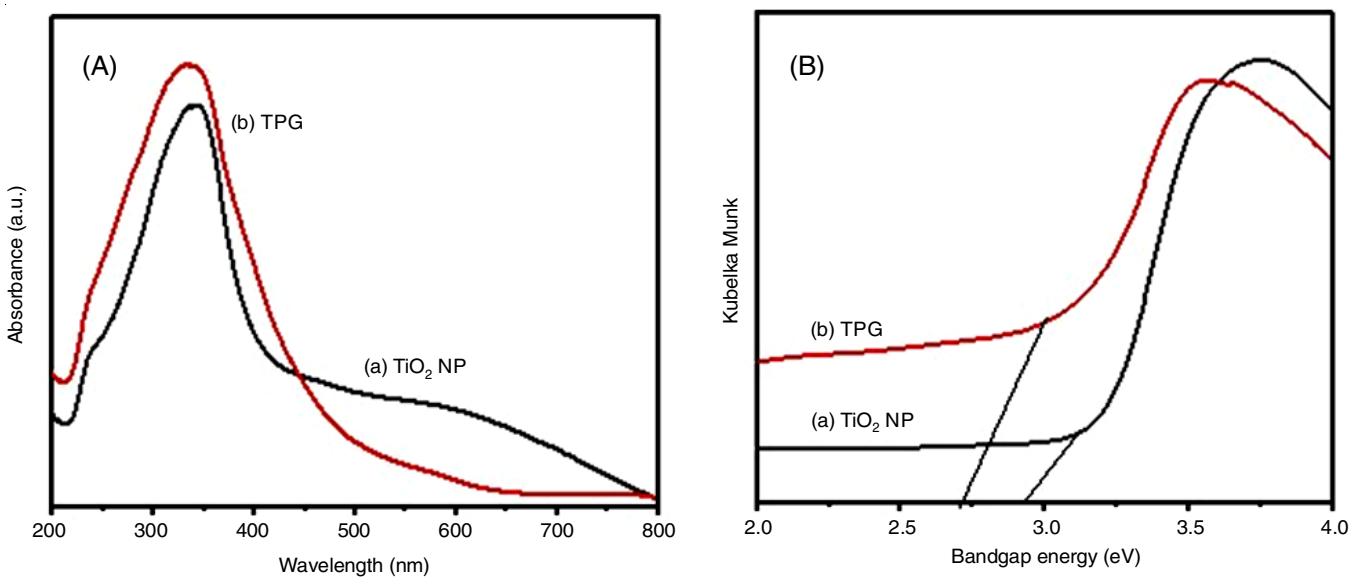

Fig. 4. (A) UV-Vis DRS plot and (B) Kubelka Munk plot of (a) TiO_2 NP and (b) TPG

(Fig. 5). A peak shift towards red wavelength and its indicative of increased particle size, whereas PL intensity was slightly decreased for TPG than with TiO_2 nanoparticles, which clearly indicates lower recombination rate for PEGylated TiO_2 nanocomposite.

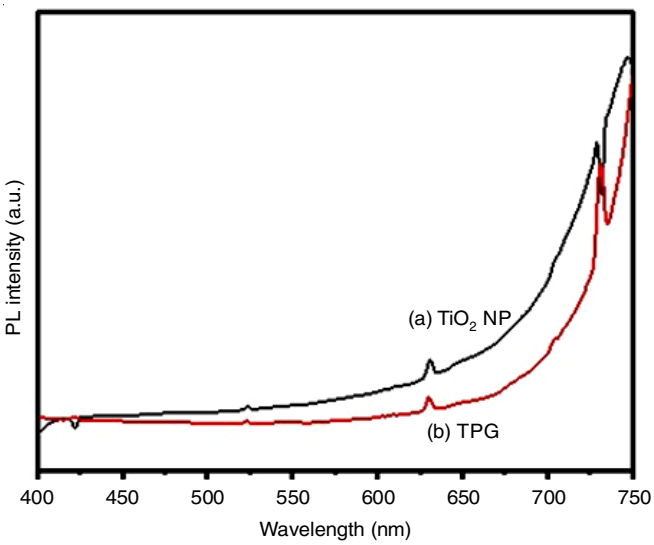

Fig. 5. Photoluminiscence spectra of (a) TiO_2 NP and (b) TPG

BET surface area: Surface areas of the catalysts were measured using BET-method by performing N_2 physical adsorption-desorption method. TPG nanocomposite as catalyst exhibited higher surface area (151 m^2/g) as compared to nano-TiO_2 (57 m^2/g) due to well dispersed TiO_2 nanoparticles in the PEG matrix. Adsorption isotherms of both catalysts in the present study are shown in Fig. 6.

FTIR studies: Fig. 7 shows the FTIR spectra of both catalysts (TiO_2 NPs and TGP). FTIR spectrum clearly shows prominent peaks corresponding to TiO_2 NPs. The first broad band at region 3600-3000 cm^{-1} is due to O-H stretching mode of the hydroxyl group [27,28]. The peak at 1740 cm^{-1} is characteristic of C=O bending mode of vibration where as peaks at 1217 cm^{-1} and 1367 cm^{-1} are related to the C-O stretching vibration, respectively. Band from the region 781cm^{-1} to 896 cm^{-1} corresponds to Ti-O-Ti streching vibration [29].

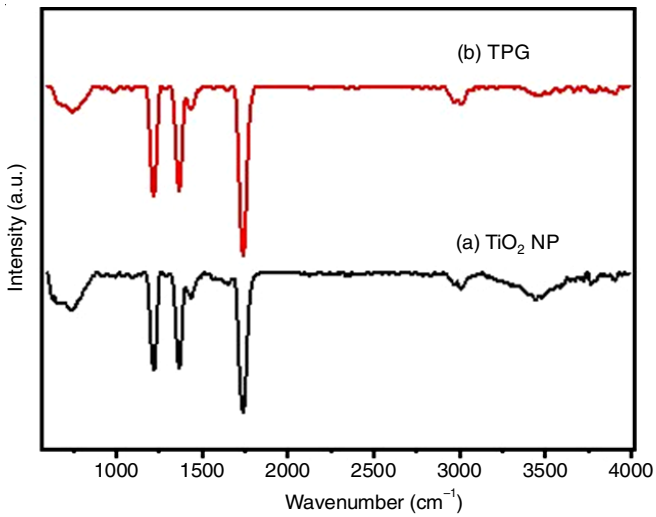

Fig. 7. FTIR spectra of the catalysts (a) TiO_2 NP and (b) TPG

Raman studies: Raman spectra of the prepared TiO_2 NPs and TPG are shown in Fig. 8. The Raman spectra of both catalysts show four peaks due to the anatase phase of TiO_2 nanoparticles [30]. Bands in the region of 600-400 cm^{-1} in TiO_2-PEG are in good agreement with the Raman active vibrational modes of titania that proves structure of TiO_2 was not altered even with addition of PEG [31]. The Raman peaks identified at 162 cm^{-1}, 401 cm^{-1}, 519 cm^{-1} and 643 cm^{-1} correspond to E_g, B_{1g}, A_{1g} and E_g active modes in TiO_2.

X-ray photoelectron spectral (XPS) studies: Fig. 9 shows the typical XPS spectra of TiO_2 NPs and TPG, which indicated that the nanomaterials are mainly composed of Ti, O and C elements. The XPS spectra of catalysts indicated two signals at 458.5 & 461 eV (Ti $2p_{3/2}$) and 462.4 & 466.7 eV (Ti $2p_{1/2}$)

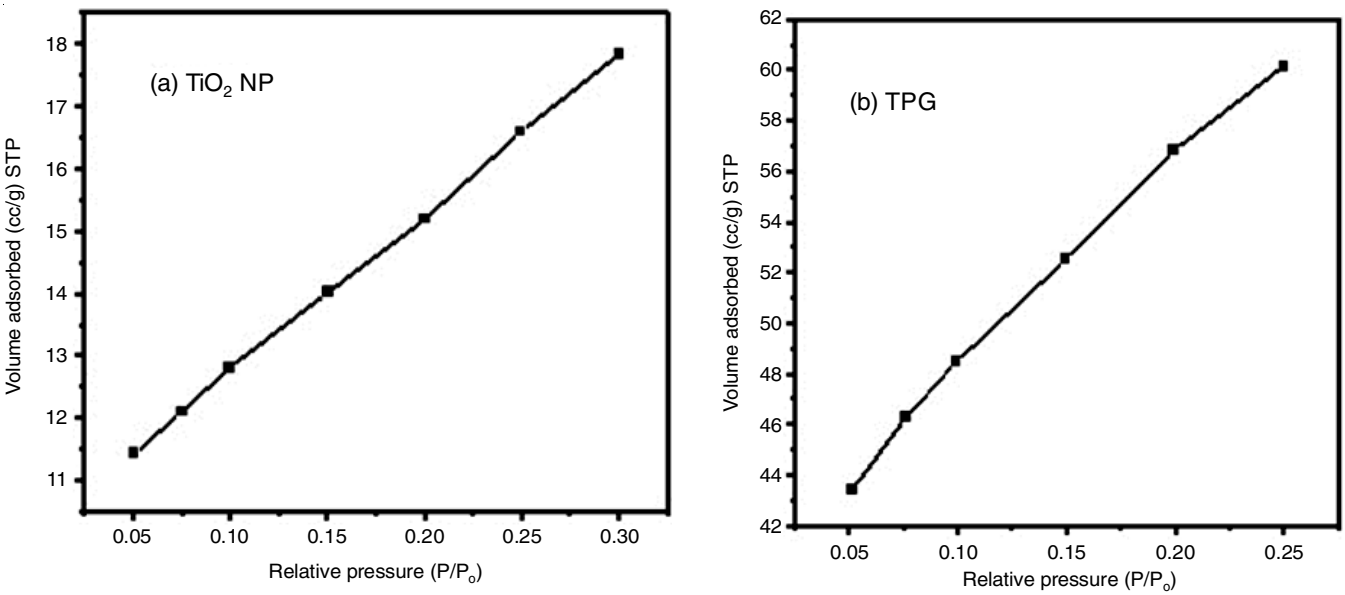

Fig. 6. N_2 adsorption and desorption isotherm of (a) TiO_2 NP and (b) TPG

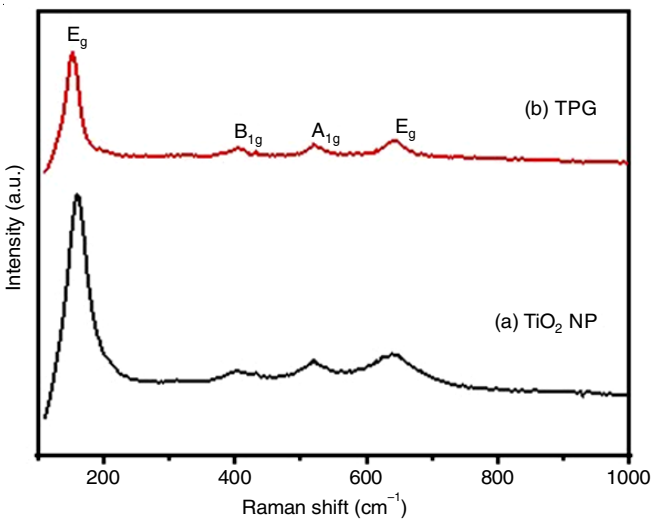

Fig. 8. Raman spectra of (a) TiO_2 NP and (b) TPG

of TiO_2 NPs and TPG respectively in accordance with the binding energy of Ti^{4+} in the database of TiO_2. Titania existed at the surface in the state Ti^{4+} converts to Ti^{3+} by trapping photogenerated electrons [32]. The O 1*s* showed binding energy at 530.5 eV & 532.3 eV with TiO_2 NPs and TPG, respectively and C 1*s* was found at 286.4 eV in case of TPG.

Photocatalytic activity: The catalytic activity of TiO_2 NPs and TiO_2-PEG nanocomposite (TPG) was examined by studying the degradation of ciprofloxacin (CIP) and norfloxacin (NOR) under visible and solar light irradiation. A 500 ppm each of ciprofloxacin and norfloxacin solutions were prepared by dissolving 100 mg in 0.1 M NaCl solution. Then, it is diluted to 250 ppm using phosphate buffer pH of 7. The mother solution was scanned in the range of 200 to 800 nm to record maximum wavelength using a UV-visible spectrophotometer. Photocatalysis in the presence of catalysts was performed in visible light under different experimental conditions such as optimized pH using phosphate buffer, different antibiotic concentration and catalyst dosage.

The concentration of CIP and NOR between 20, 50 and 75 mg/L with optimum amounts of TiO_2 nanoparticles and TiO_2-PEG nanocomposite of 20, 50 and 75 mg were run separately at time intervals of 30 min till 180 min to record the steady state activities. Their absorbances were measured at maximum wavelength of 270 nm. The degradation activity was found to be higher at 50 mg/L concentration of drug solution with 75 mg of catalyst at degradation time of 180 min. In sunlight, the photocatalytic degradation of ciprofloxacin and norfloxacin was also evaluated separately by using 100 mL of variable amounts of drug solution with the catalysts dosage. The degradation activity was found to be higher at 20 mg/L concentration of drug solution with 50 mg of catalyst at degradation time of 180 min. The photocatalysts, TiO_2 NPs and TiO_2-PEG nanocomposite showed 65% and 74%, respectively of degradation of ciprofloxacin in visible light irradiation, whereas the degradation efficiency was 57% and 65% for norfloxacin. The degradation efficiency for ciprofloxacin in sunlight was found to be 77% with TiO_2 NPs whereas it was 80.2% with catalyst TPG similarly for norfloxacin degradation efficiency with TiO_2 NPs was found to be 68.6% and with TPG it was 78.7%, respectively (Fig. 10a-h). However, this study reported that surface modified PEGylated TiO_2 nanocomposite showed high degradation for both antibiotics under visible and sunlight than unmodified pure TiO_2 nanoparticles.

Kinetic studies: An apparent psuedo first-order reaction kinetics through a Langmuir-Hinshelwood mechanism is observed in this regard. The percentage degradation with time curve for all the reactions and graph of ln C/C_o *vs*. time are displayed in Figs. 11 and 12 in visible and sunlight irradiation, respectively. The results (Table-1) report that degradation rates were higher over TPG compared with TiO_2 NPs for both ciprofloxacin and norfloxacin. And also, the rates of degradation of these antibiotics were slightly higher in presence of sunlight as compared to visible light irradiation. The photodegradation rate over TPG was found to be much higher than some of the reported catalysts at higher concentrations of the antibiotics [33].

TABLE-1
% DEGRADATION AND RATE CONSTANTS OF ANTIBIOTICS OVER TiO_2 CATALYSTS

Antibiotic	Catalyst	Degradation (%)	Rate constant k (min^{-1}) × 10^{-3}
Ciprofloxacin in visible light	TiO_2 NP	65.0	7.5
	TPG	74.0	8.7
Norfloxacin in visible light	TiO_2 NP	57.0	7.0
	TPG	64.0	7.4
Ciprofloxacin in sun light	TiO_2 NP	77.0	8.9
	TPG	80.2	9.1
Norfloxacin in sun light	TiO_2 NP	68.6	7.7
	TPG	78.7	9.0

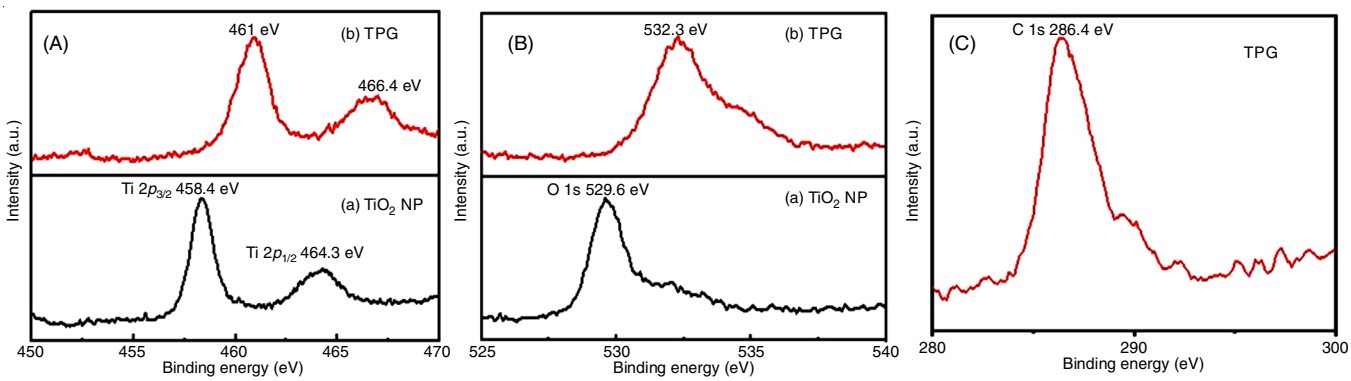

Fig. 9. XPS spectra of the TiO_2 catalysts of (A) Ti 2p (B) O 1s and (C) C 1s

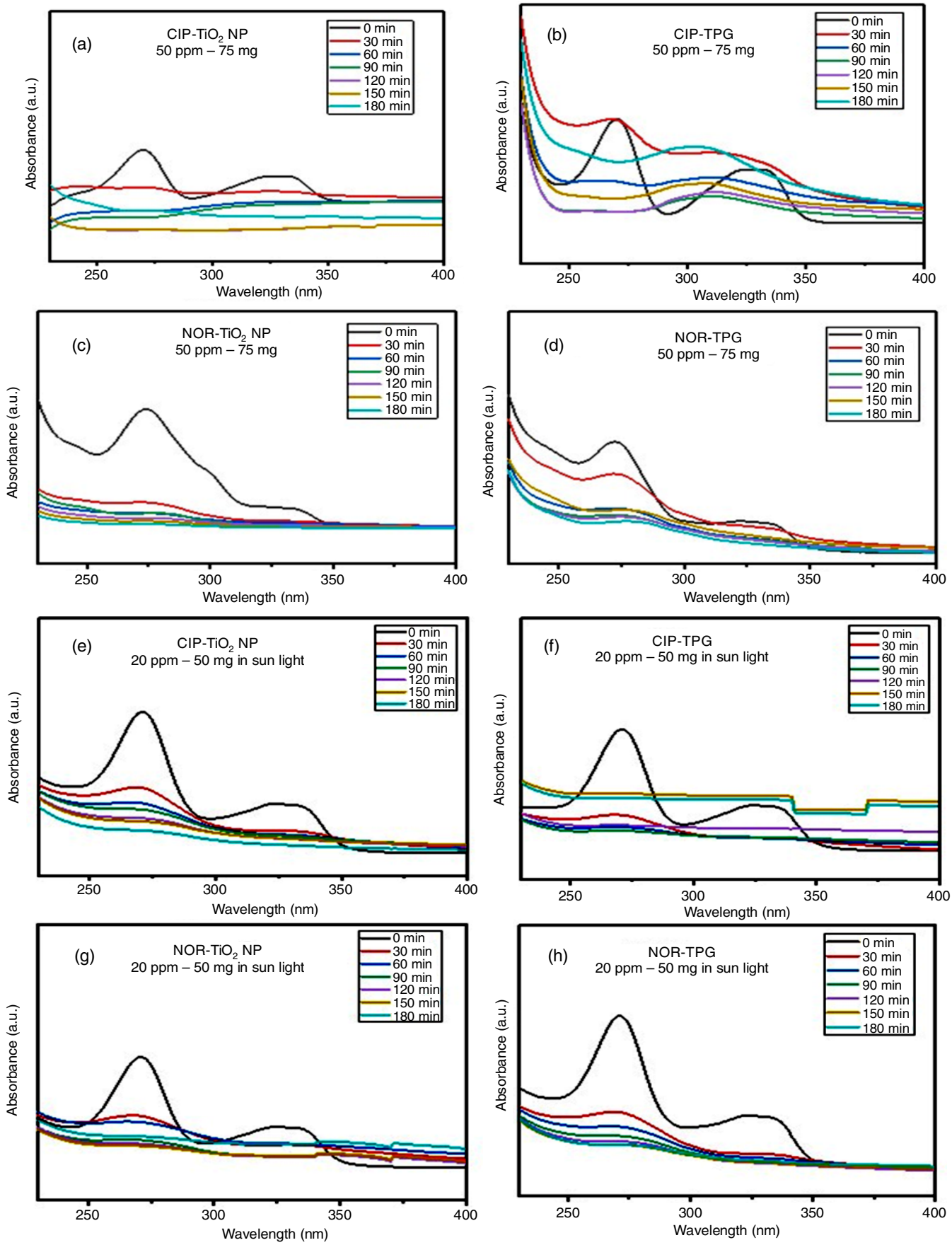

Fig. 10. UV-VIS absorption spectra of (a-d) 50 ppm of ciprofloxacin and norfloxacin over 75 mg catalysts in visible light; (e-h) 20 ppm of ciprofloxacin and norfloxacin over 50 mg catalysts in sun light

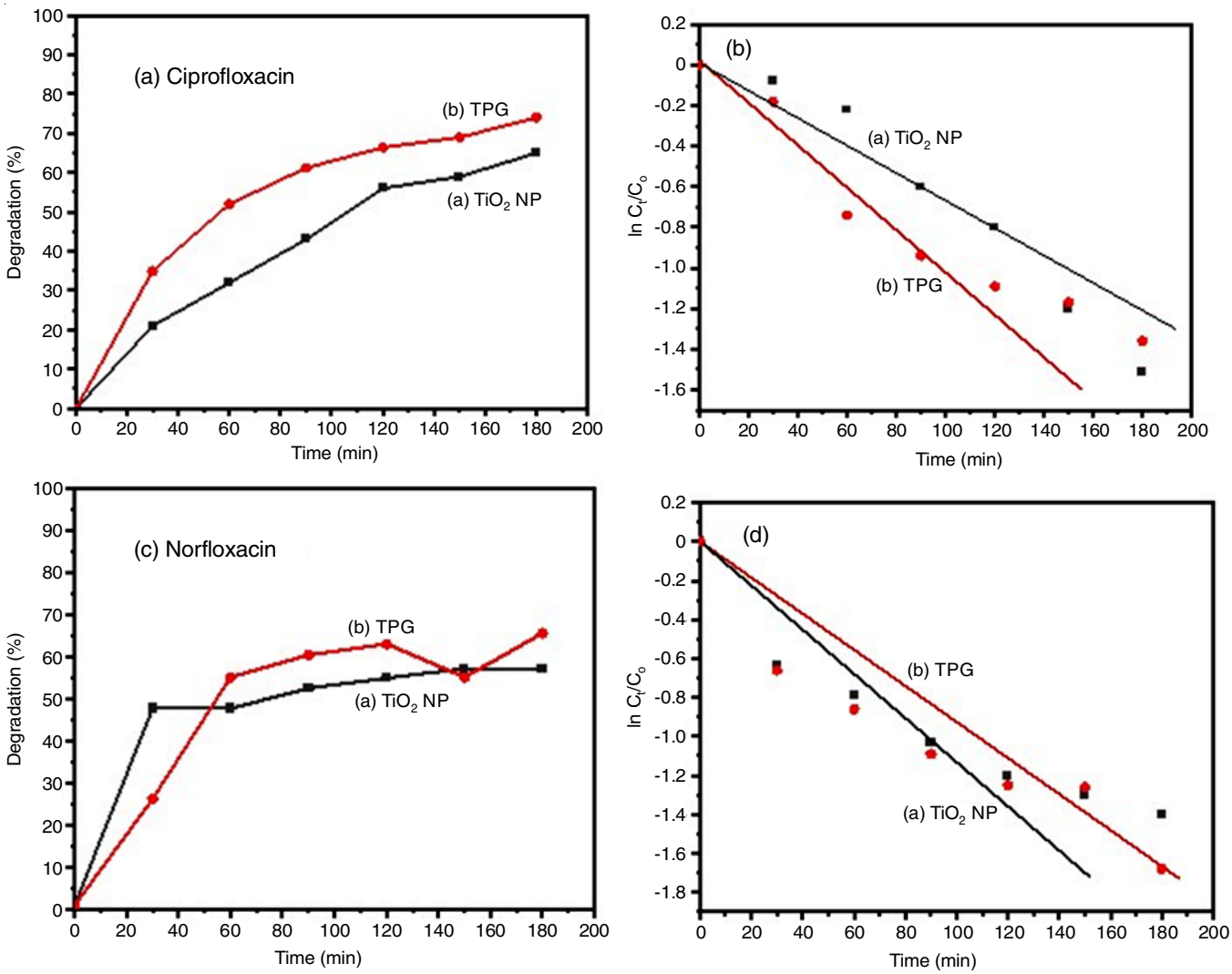

Fig. 11. Time on stream study of % degradation and ln C/C_o *vs.* time graph of the catalysts for ciprofloxacin and norfloxacin in visible light irradiation

Regeneration studies: Recycling experiments were also performed to access photocatalytic performance of TiO_2 NPs and TPG over different photocatalytic cycles selecting ciprofloxacin as common antibiotic. After each cycle the catalysts were rinsed with distilled water, dried and reused under identical conditions to test their activity. It can be clearly observed from Fig. 13 that even after 5 cycles of use, the activity of the catalysts was mostly retained thus indicating the stability of the catalysts.

Reaction mechanism: Under UV irradiation the electrons of TiO_2 nanoparticles (catalyst) are stimulated and transferred from valence band (VB) to the conduction band (CB) [34]. This generates electron-hole pair over the surface of the photocatalyst. Then the photogenerated electrons were captured directly by the O_2 forming superoxide radicals ($O_2^{\bullet -}$), meanwhile the positively charged holes (h^+) reach the surface and react with surface water (H_2O) leading to the formation of hydroxyl radical ($OH^\bullet$) adsorbing hydroxyl groups (OH^-). The hydroxyl radicals thus formed react with each other generating hydrogen peroxide (H_2O_2) [35]. These reactive oxygen species (ROS) generated would decompose the contaminant into CO_2, H_2O and other degradation products. The whole process can be explained in the form of the following equations:

$$\text{Catalyst} + h\nu \longrightarrow e^- + h^+ \quad (1)$$

$$h^+ + H_2O \longrightarrow H^+ + OH^\bullet \quad (2)$$

$$h^+ + OH^- \longrightarrow OH^\bullet \quad (3)$$

$$e^- + O_2 \longrightarrow O^{2-} \quad (4)$$

$$2e^- + O_2 + 2H^+ \longrightarrow H_2O_2 \quad (5)$$

$$e^- + H_2O_2 \longrightarrow OH^\bullet + OH \quad (6)$$

$$\text{CIP/NOR} + {}^\bullet OH + O_2 \longrightarrow CO_2 + H_2O + \text{other degraded products} \quad (7)$$

Scavenger study in support of reaction mechanism: Scavenger study clearly supports the reaction mechanism with the best catalyst photocatalytic activity using hydroxyl radical, superoxide radical and hole scavengers such as formic acid, benzoquinone and isopropyl alcohol. The results indicated that photocatalytic activity was greatly inhibited by the addition of benzoquinone thus implying the superoxide radicals as the

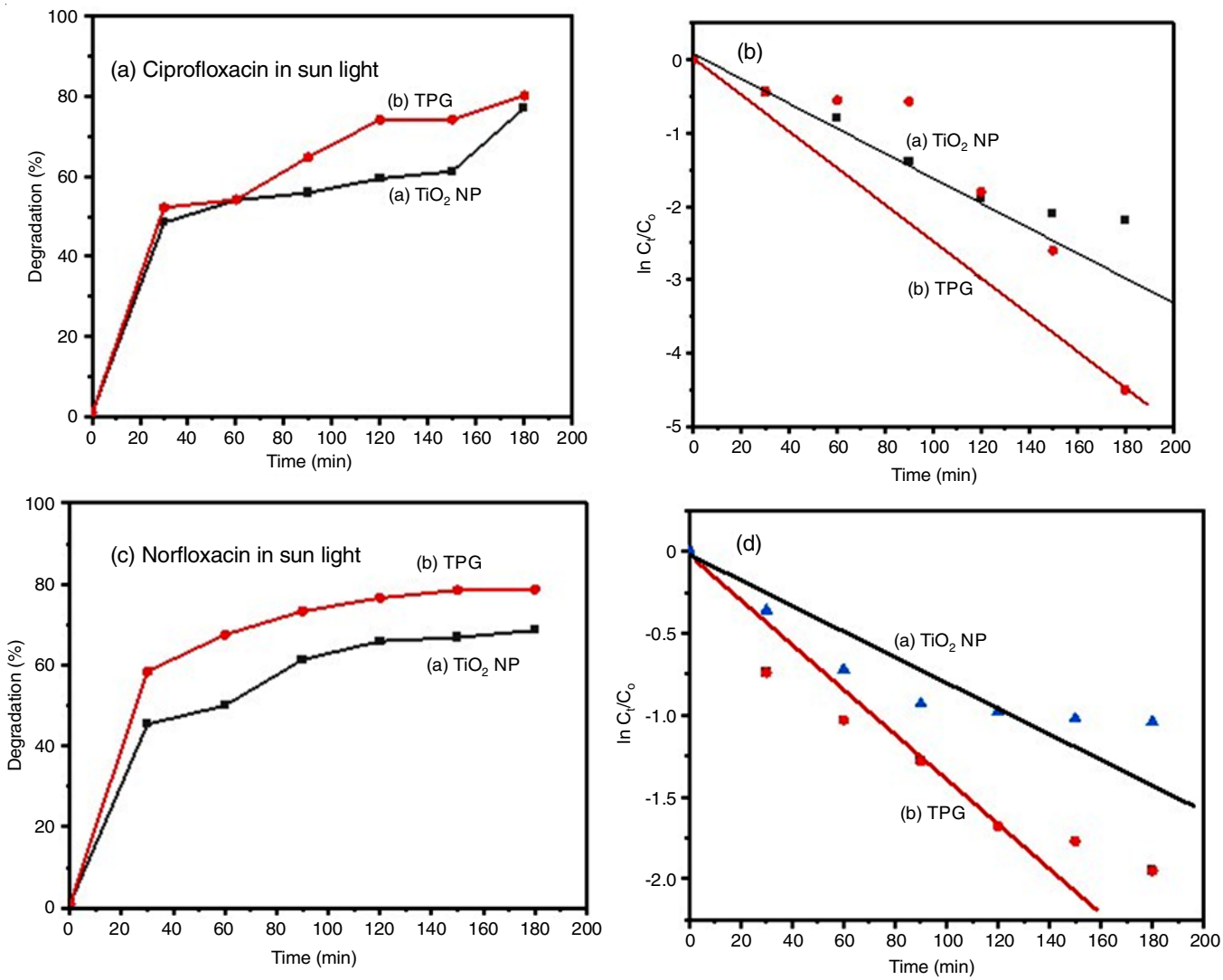

Fig. 12. Time on stream study of % degradation and ln C/C_o *vs*. time graph of the catalysts for ciprofloxacin and norfloxacin in sun light irradiation

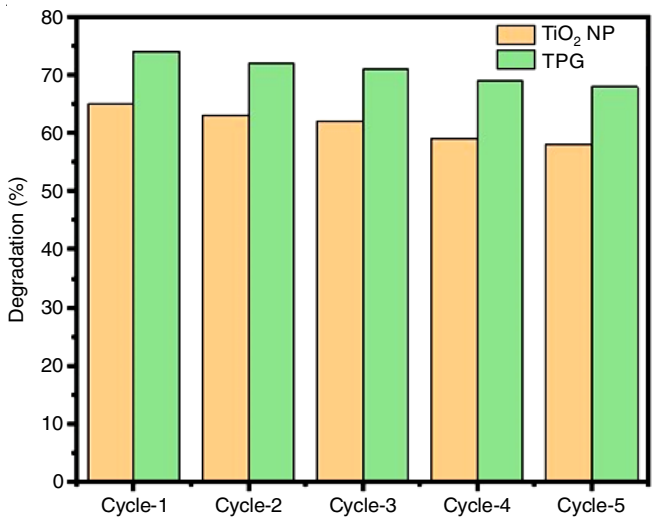

Fig. 13. Reusability of photocatalysts, TiO_2 NP and TPG

main reactive species in this reaction mechanism. Contribution of each reactive species on degradation of ciprofloxacin was shown with the following decreasing order $O_2^{\bullet-} > OH^- > h^+ >$ no scavenger.

The study clearly demonstrates the potential of TPG as an efficient catalyst for photodegradation of ciprofloxacin and norfloxacin. The enhanced surface area of TiO_2 nanocomposite leading to higher dispersion and uniform particle size distribution in nanoscale seems to further decrease the band gap and electron-hole pairs recombination rates that are responsible for the efficient photodegradation rates of TPG. Further since the PEGlyation can enhance the adsorption of the antibiotic and stability of the nanoparticles of TiO_2, it seems to play an advantageous role in the enhanced activity of the nanocomposite over its counterpart TiO_2 nanoparticles.

Conclusion

In this work, TiO_2 nanoparticles and PEG modified TiO_2 nanocomposite synthesized by sol-gel method were used in the study of photocatalytic degradation of two antibiotics *viz*. ciprofloxacin and norfloxacin belonging to the fluoroquinolone family in visible light and sun light irradiation. The nanocom-

posite sample was found to be advantageous and more efficient over TiO_2 nanoparticles in the photocatalytic degradation of both antibiotics. Both catalysts showed only anatase phase with nanocrystallites from the XRD analysis with PEG modified titania nanocomposite showing least crystallite size about 14.93 nm. Surface area measurements by BET clearly indicated the enhanced surface generation with PEGylation as a result of more dispersed particles that were prevented from agglomerization. The UV-DRS data indicated greater reduction in band gap energy for PEG modified catalyst than unmodified TiO_2 NP. A sharp and broad range of emission spectra was confirmed by photoluminescence that exhibits lower recombination rate for TPG catalyst. Among both catalysts, TPG nanocomposite showed high efficiency in degradation of both antibiotics in visible and sunlight irradiation.

ACKNOWLEDGEMENTS

The authors thank OU-DST-PURSE II and OU-UGC-SAP-DRS-II for the financial support and Prof. M. Vithal, Emeritus Scientist, Department of Chemistry, Osmania University, Hyderabad, India for permitting to use his laboratory equipment. The authors also thank Dr. A. Venugopal, Chief Scientist, and Dr. L. Giribabu, Senior Principal Scientist, CSIR-IICT, Hyderabad, India for extended support in some of the characterization of catalysts.

CONFLICT OF INTEREST

The authors declare that there is no conflict of interests regarding the publication of this article.

REFERENCES

1. R. Kumar, J. Travas-Sejdic and L.P. Padhye, *Chem. Eng. J. Adv.*, **4**, 100047 (2020); https://doi.org/10.1016/j.ceja.2020.100047
2. I.-Y. Jeon and J.-B. Baek, *Materials*, **3**, 3654 (2010); https://doi.org/10.3390/ma3063654
3. V.V. Vodnik, J.V. Vukovic and J.M. Nedeljkovic, *Colloid Polym. Sci.*, **287**, 847 (2009); https://doi.org/10.1007/s00396-009-2039-7
4. C.I. Pearce, J.R. Lloyd and J.T. Guthrie, *Dyes Pigments*, **58**, 179 (2003); https://doi.org/10.1016/S0143-7208(03)00064-0
5. B. Van Der Bruggen and C. Vandecasteele, *Environ. Pollut.*, **122**, 435 (2003); https://doi.org/10.1016/S0269-7491(02)00308-1
6. J. Hollender, S.G. Zimmermann, S. Koepke, M. Krauss, C.S. McArdell, C. Ort, H. Singer, U. von Gunten and H. Siegrist, *Environ. Sci. Technol.*, **43**, 7862 (2009); https://doi.org/10.1021/es9014629
7. C.Y. Hu, S.L. Lo and W.H. Kuan, *Water Res.*, **37**, 4513 (2003); https://doi.org/10.1016/S0043-1354(03)00378-6
8. M. Iram, C. Guo, Y. Guan, A. Ishfaq and H. Liu, *J. Hazard. Mater.*, **181**, 1039 (2010); https://doi.org/10.1016/j.jhazmat.2010.05.119
9. C. Vanlalhmingmawia, D. Tiwari and D.-J. Kim, *Environ. Res.*, **218**, 115007 (2023); https://doi.org/10.1016/j.envres.2022.115007
10. J. Zhang, Y. Chen, J. Liang and H. Xu, *Environ. Eng. Res.*, **28**, 220513 (2023); https://doi.org/10.4491/eer.2022.513
11. P.S. Saud, B. Pant, A.M. Alam, Z.K. Ghouri, M. Park and H.Y. Kim, *Ceram. Int.*, **41**, 11953 (2015); https://doi.org/10.1016/j.ceramint.2015.06.007
12. E. Friedler and Y. Gilboa, *Sci. Total Environ.*, **408**, 2109 (2010); https://doi.org/10.1016/j.scitotenv.2010.01.051
13. Y. Choi, T. Umebayashi and M. Yoshikawa, *J. Mater. Sci.*, **39**, 1837 (2004); https://doi.org/10.1023/B:JMSC.0000016198.73153.31
14. T. Ohno, M. Akiyoshi, T. Umebayashi, K. Asai, T. Mitsui and M. Matsumura, *Appl. Catal. A Gen.*, **265**, 115 (2004); https://doi.org/10.1016/j.apcata.2004.01.007
15. P. Wang, D. Wang, H. Li, T. Xie, H. Wang and Z. Du, *J. Colloid Interface Sci.*, **314**, 337 (2007); https://doi.org/10.1016/j.jcis.2007.05.087
16. A.S. Karakoti, S. Das, S. Thevuthasan and S. Seal, *Angew. Chem. Int. Ed.*, **50**, 1980 (2011); https://doi.org/10.1002/anie.201002969
17. M. Bustamante-Torres, D. Romero-Fierro, B. Arcentales-Vera, S. Pardo and E. Bucio, *Polymers*, **13**, 2998 (2021); https://doi.org/10.3390/polym13172998
18. J.S. Suk, Q. Xu, N. Kim, J. Hanes and L.M. Ensign, *Adv. Drug Deliv. Rev.*, **99**, 28 (2016); https://doi.org/10.1016/j.addr.2015.09.012
19. Z. Zheng, Q. Zhou, M. Li and P. Yin, *Chem. Sci.*, **10**, 7333 (2019); https://doi.org/10.1039/C9SC02779C
20. X. Yan, D. Pan, Z. Li, Y. Liu, J. Zhang, G. Xu and M. Wu, *Mater. Lett.*, **64**, 1833 (2010); https://doi.org/10.1016/j.matlet.2010.05.051
21. M. Zhang, J. Lei, Y. Shi, L. Zhang, Y. Ye, D. Li and C. Mu, *RSC Adv.*, **6**, 83366 (2016); https://doi.org/10.1039/C6RA12988A
22. L.N. Costa, F.X. Nobre, A.O. Lobo and J.M.E. de Matos, *Environ. Nanotechnol. Monit. Manag.*, **16**, 100466 (2021); https://doi.org/10.1016/j.enmm.2021.100466
23. M. Behpour and M. Chakeri, *J. Nanostructures*, **02**, 227 (2012); https://doi.org/10.7508/jns.2012.02.011
24. S. Rahim, M.S. Ghamsari and S. Radiman, *Sci. Iran.*, **19**, 948 (2012); https://doi.org/10.1016/j.scient.2012.03.009
25. S. Sood, S.K. Mehta, A. Umar and S.K. Kansal, *New J. Chem.*, **38**, 3127 (2014); https://doi.org/10.1039/C4NJ00179F
26. B. Subash, B. Krishnakumar, M. Swaminathan and M. Shanthi, *Langmuir*, **29**, 939 (2013); https://doi.org/10.1021/la303842c
27. A. Kathiravan and R. Renganathan, *J. Colloid Interface Sci.*, **335**, 196 (2009); https://doi.org/10.1016/j.jcis.2009.03.076
28. K. Olurode, G.M. Neelgund, A. Oki and Z. Luo, *Spectrochim. Acta A Mol. Biomol. Spectrosc.*, **89**, 333 (2012); https://doi.org/10.1016/j.saa.2011.12.025
29. J. Wei, L. Zhao, S. Peng, J. Shi, Z. Liu and W. Wen, *J. Sol-Gel Sci. Technol.*, **47**, 311 (2008); https://doi.org/10.1007/s10971-008-1787-z
30. H.C. Choi, Y.M. Jung and S.B. Kim, *Vib. Spectrosc.*, **37**, 33 (2005); https://doi.org/10.1016/j.vibspec.2004.05.006
31. A. Leon, P. Reuquen, C. Garin, R. Segura, P. Vargas, P. Zapata and P. Orihuela, *Appl. Sci.*, **7**, 49 (2017); https://doi.org/10.3390/app7010049
32. W. Wang, C.-H. Lu, Y.-R. Ni, J.-B. Song, M.-X. Su and Z.-Z. Xu, *Catal. Commun.*, **22**, 19 (2012); https://doi.org/10.1016/j.catcom.2012.02.011
33. J. Wang, L. Svoboda, Z. Nìmeèková, J. Henych, N. Licciardello, M. Sgarzi and G. Cuniberti, *RSC Adv.*, **11**, 13980 (2021); https://doi.org/10.1039/D0RA10403E
34. Y. Li, Y. Wang, J. Kong, H. Jia and Z. Wang, *Appl. Surf. Sci.*, **344**, 176 (2015); https://doi.org/10.1016/j.apsusc.2015.03.085
35. G. Ma, Y. Zhu, Z. Zhang and L. Li, *Appl. Surf. Sci.*, **313**, 817 (2014); https://doi.org/10.1016/j.apsusc.2014.06.079